Diffraction Space Mapping of Epitaxy and Strain in Multilayered Thin Film Superconductor Embodiments

K. Venkataraman,[1,2] A. J. Kropf,[1] C. U. Segre,[3] Q. Jia,[4] S. R. Foltyn,[4]
A. K. Cochran,[1] S. Chattopadhyay,[3] V. A. Maroni[1]
[1]Argonne National Laboratory, Argonne, IL, U.S.A.
[2]University of Illinois at Chicago, Chicago, IL, U.S.A.
[3]Illinois Institute of Technology, Chicago, IL, U.S.A.
[4]Los Alamos National Laboratory, Los Alamos, NM, U.S.A.

Introduction

The growth of epitaxial films of $MBa_2Cu_3O_{7-x}$ (M-123, in which M = yttrium or a rare earth element) on metal substrates is being pursued worldwide as a means of fabricating high-critical-temperature superconducting (HTS) wire (in long-length form) for electric power applications [1-3]. This approach to developing HTS structures for high-current/high-voltage devices relies on being able to transmit the cube-textured epitaxy of the substrate to the M-123 film. The substrate can be a cube-textured metal (such as nickel or a nickel-base alloy) or a metal to which a cube-textured seed layer has been applied. The fabrication of these coated conductor embodiments usually also requires a buffer layer to prevent the constituent metal atoms of the substrate from diffusing into the M-123 film. Hence, the architecture of an M-123 coated conductor typically consists of the metal substrate, a seed layer (if one is needed), a buffer layer, one or more cap layers (to enhance the epitaxy transmission), and the M-123 film. Whereas it is desirable to have the M-123 film be relatively thick (greater than a micrometer), most of the intervening layers (between the M-123 film and the metal substrate) tend to range from 10 to 100 nm in thickness. The fabrication of this multilayered epitaxial superstructure requires meticulous attention to detail at each stage of the process. In order to develop a clear understanding of these details, it is critically important to be able to measure the texture and strain characteristics at each interface. This report summarizes recent work done at the APS that employs the technique of high-resolution diffraction space mapping [4] to measure the texture, interplanar tilt, degree of orthorhombicity, and strain field pattern in M-123 coated conductor specimens.

Methods and Materials

The Eu-123 and Er-123 films on $SrTiO_3$(100) single-crystal substrates reported on in this report were prepared by pulsed laser deposition (PLD) from $EuBa_2Cu_3O_{7-x}$ and $ErBa_2Cu_3O_{7-x}$ targets [5]. Reported lattice parameters for these three materials [6] are listed in Table 1.

Table 1. Lattice parameters: Eu-123, Er-123, and $SrTiO_3$.

Material*	**a** (nm)	**b** (nm)	**c** (nm)
Eu-123^{O}	0.384	0.390	1.171
Eu-123^{T}	0.388	0.388	1.181
Er-123^{O}	0.382	0.389	1.169
Er-123^{T}	0.385	0.385	1.178
$SrTiO_3$	0.390	0.390	0.390

*****The O and T superscripts refer to the orthorhombic and tetragonal structures, respectively.

The measurements were made at the APS on the Materials Research Collaborative Access Team (MR-CAT) insertion device beamline (10-ID), which is equipped with an eight-circle Huber diffractometer. The diffraction patterns were recorded by using an x-ray energy of 17 keV (0.72928 Å). The beam spot on the sample was slitted to a 2×1-mm rectangle. An Si(111) crystal analyzer was inserted between the sample and the detector to enhance the resolution.

Results and Discussion

High-resolution diffraction space maps (DSMs) were recorded for three specimens: (1) about 160-nm-thick Eu-123 film on (100) $SrTiO_3$ (STO), (2) about 160-nm-thick Eu-123 film on (100) STO that was precoated with about 10 nm of Er-123, and (3) a clean (100) STO single-crystal specimen (to sort out substrate-related effects). The first Eu-123/STO specimen showed no evidence of a critical temperature (Tc) above 75K, while the second Eu-123/Er-123/STO specimen had a Tc of 92.5K and exhibited a critical current density of 2.1 MA/cm^2. DSMs (2-θ versus ω) for the two M-123 coated specimens are shown in Fig. 1. Included in Fig. 1 are maps for the diffraction space domains of three reflections: (1) the (200) reflections of the STO substrate for the Eu-123/STO and Eu-123/Er-123/STO specimens, which also encompass the (006) reflections of the M-123 phases [Figs. 1(a) and 1(b)]; (2) the (005) reflections of the M-123 phases [Figs. 1(c) and 1(d)]; and (3) the

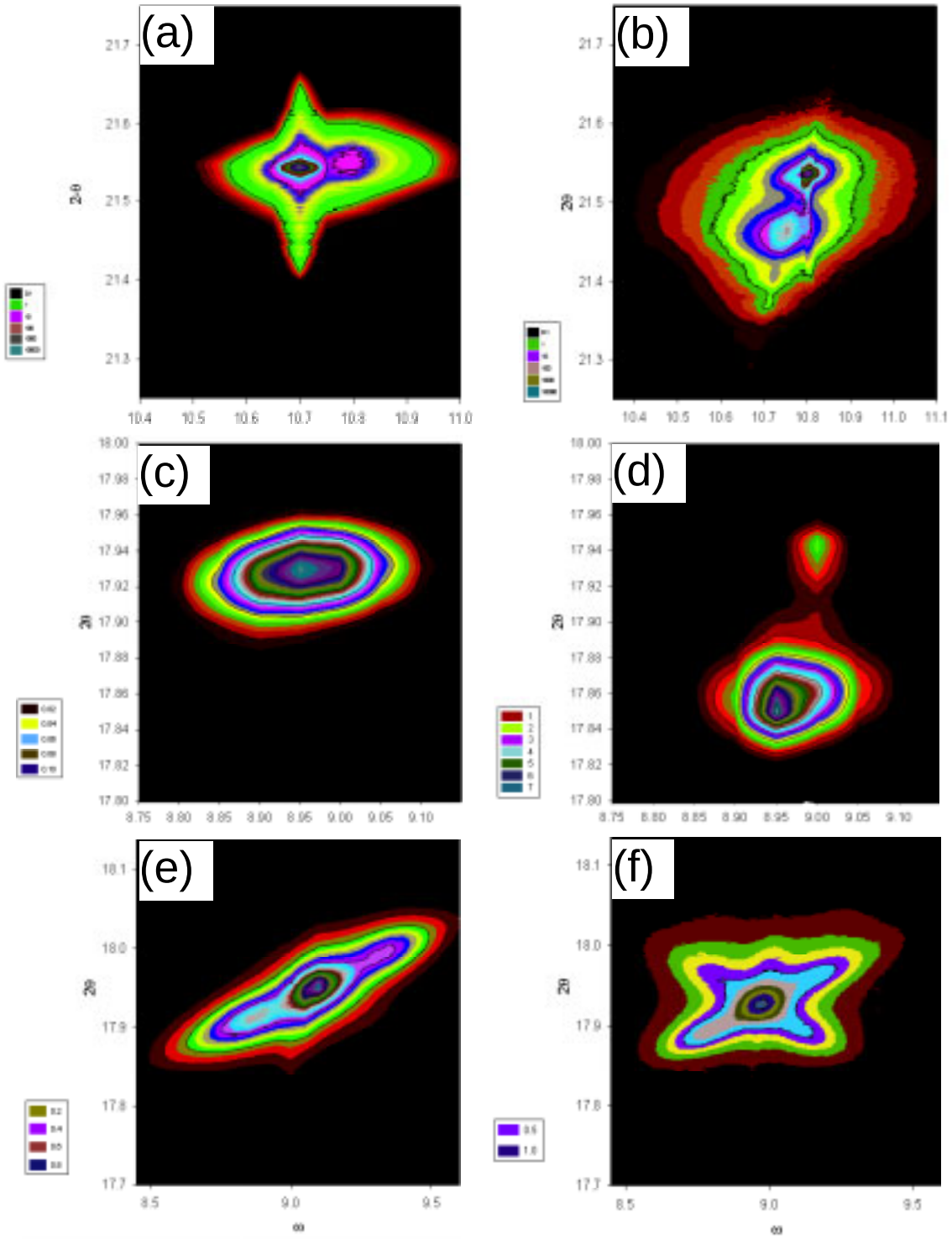

FIG. 1. DSMs. Intensity projections are logarithmic for (a) and (b) and linear for (c) through (f).
(a) DSM for the region of the STO (200) and Eu-123 (006) reflections of the Eu-123/STO specimen.
(b) DSM for the region of the STO (200) and M-123 (006) reflections of the Eu-123/Er-123/STO specimen.
(c) DSM for the region of the Eu-123 (005) reflection of the Eu-123/STO specimen.
(d) DSM for the region of the M-123 (005) reflection of the Eu-123/Er-123/STO specimen.
(e) DSM for the region of the Eu-123 (104)/(014) reflections of the Eu-123/STO specimen.
(f) DSM for the region of the M-123 (104)/(014) reflections of the Eu-123/Er-123/STO specimen.

(104)/(014) reflections of the M-123 phases [Figs. 1(e) and 1(f)].

The **a** and **b** lattice parameters for orthorhombic and tetragonal Eu-123 and Er-123 match the lattice constant of cubic STO (0.390 nm) within 0.01 nm, but their **c** axis parameters are considerably larger (>1.1 nm). For this reason, M-123 films tend to grow cube-on-cube on (100) STO with the **a**-**b** planes parallel to the substrate surface and the **c** axis perpendicular to it. The measured lattice parameters for epitaxial M-123 films on textured substrates are primarily determined by two generally unrelated properties: the oxygen content of the M-123 phase and the interface characteristics that create strain. In the case of the Eu-123/STO specimen, the (006) reflection of Eu-123 appears at nearly the same 2-θ value as the (200) reflection of STO [intense center spot in Fig. 1(a)] but at a slightly higher ω value [weak side spot in Fig. 1(a)]. This is corroborated by the value of the (005) reflection in Fig. 1(c), which equates to an Eu-123 **c** axis lattice parameter of 1.170 nm (i.e., exactly three times the STO lattice parameter and only 0.001 nm less than the **c** value for unstrained, orthorhombic Eu-123; see Table 1). The small ω displacement of the Eu-123 (006) reflection is most probably the result of a slight interplanar tilt of the Eu-123 film relative to the STO surface.

In the case of the Eu-123/Er-123/STO specimen, the (006) reflection of the thin Er-123 film is presumed to fall on the (200) of STO in Fig. 1(b) since it also produces the weaker (005) spot near 2-θ = 17.94^{o} in Fig. 1(d). Thus, it seems to match to STO (200) in the same way that the Eu-123 film does in the Eu-123/STO specimen. However, the Eu-123 film on top of the Er-123/STO substrate exhibits (006) and (005) reflections at lower 2-θ values than did the Eu-123 on STO specimen [see Figs. 1(a) and 1(b) and Figs. 1(c) and 1(d)]. The elucidation of this restructuring of the Eu-123 lattice in the presence of the Er-123 underlayer, as it relates to oxygen stoichiometry, cation disorder, and interfacial strain, is in progress.

Of greatest significance, however, are the differences in the (104)/(014) diffraction space maps for the two specimens [Figs. 1(e) and 1(f)]. The Eu-123 film directly on STO appears to contain a single spot [Fig. 1(e)], indicating near-equivalence of the (104) and (014) lattice diffraction spacings and presumably therefore near-equivalence of the Eu-123 **a** and **b** lattice parameters, which is suggestive of a tetragonal lattice. It is clear from Table 1 that a tetragonal Eu-123 lattice would fit better on (100) STO than would an orthorhombic one, because, on average, **a** and **b** of Eu-123^{T} fit better on STO than do **a** and **b** of Eu-123^{O}. In the case of the Eu-123/STO specimen, the oxygenation treatment given the sample should have produced orthorhombic Eu-123. Hence, we suspect that the STO substrate is forcing the Eu-123 into an oxygen-disordered structure, which might explain the absence of a Tc above 75K. The diagonal streaking of the diffraction spot in Fig. 1(e) is attributable to a combination of strain field variation and elemental (cation and/or oxygen) disorder in the lattice [4]. The relative importance and magnitudes of these two phenomena are currently under investigation.

For the Eu-123/Er-123/STO specimen, we find two spots in the Eu-123 (104)/(014) diffraction space map (Fig. 1f) that cross diagonally, suggesting that the Eu-123^{O} film in this specimen is twinned and influenced by strain and disorder as well. Seemingly, the thin Er-123 film does not transmit the straining influence of the (100) STO substrate to the Eu-123 film. Interestingly, the Eu-123 (006) and (005) diffraction space maps [Figs. 1(a)-1(d)] exhibit a spreading in the ω direction that is indicative of nanoscale misalignments in the Eu-123 mosaic [4]. Of most importance for this work will be the correlation of the diffraction space results with Tc and critical current properties of M-123 coated conductors.

Acknowledgments

This research was sponsored by the U.S. Department of Energy (DOE), Office of Energy Efficiency and Renewable Energy. Use of the APS was supported by the DOE Office of Science, Office of Basic Energy Sciences (BES), under Contract No. W-32-109-ENG-38. All aspects of the research were performed under this contract. The MR-CAT beamlines are supported by the member institutions and by DOE BES under Contract Nos. DE-FG02-94ER45525 and DE-FG02-96ER-45589.

References

[1] D. Larbalestier, A. Gurevich, D. M. Feldmann, and A. Polyanskii, Nature **414**, 368-377 (2001).

[2] Y. Iijima and K. Matsumoto, Supercon. Sci. Technol. **13**, 68-81 (2000).

[3] D. K. Finnemore, K. E. Gray, M. P. Maley, D. O. Welch, D. K. Christen, and D. M. Kroeger, Phys. C **320**, 1-8 (1999).

[4] P. F. Fewster, Crit. Rev. Solid State **22**(2), 69-110 (1997).

[5] Q. X. Jia, X. D. Wu, S. R. Foltyn, P. Tiwari, Appl. Phys. Lett. **66**, 2197-2199 (1995).

[6] Joint Committee on Powder Diffraction (JCPDS), International Center for Diffraction Data (ICDD), powder diffraction data file/CD-ROM, PDF Nos. 86-0473, 82-2303, 88-2254, 82-2308, and 86-0179 (Newton Square, PA, 1993-).